Mold flux entrainment mechanisms

Lance C HIBBELER and Brian G THOMAS

Department of Mechanical Science and Engineering, University of Illinois at Urbana-Champaign, Urbana, Ill. 61802 USA

Abstract: This paper presents a comprehensive and critical review of mold flux entrainment mechanisms in continuous casting of steel. Entrainment introduces inclusions into the final product, and thus greatly hinders clean steel production. By understanding the mechanisms that cause entrainment, the operating conditions of casters can be tuned to reduce the number of defects. Nine different mechanisms have been proposed over the last three decades, including vortex formation around the submerged entry nozzle (SEN), argon bubble interactions with the slag layer, shear-layer instability at the slag-steel interface, excessive upward flow impingement upon the meniscus, top surface level fluctuations, meniscus freezing and hook formation, top surface "balding", top surface standing wave instability, and slag crawling down the SEN. The previous work done for each of these mechanisms is presented, including both quantitative and qualitative descriptions of their behavior.

Key words: mold flux entrainment; inclusions; clean steel production

1 Introduction

Mold flux/slag entrainment, also called emulsification, entrapment, involvement, or engulfment is an important problem in the production of clean steel. By any name, this phenomenon of interest in this work is characterized by droplets of melted mold powder being drawn into the molten steel pool inside a continuous casting mold. Mold flux entrainment can cause both surface and internal defects if the entrained particles become trapped in the solidifying steel. All of the previous work on this subject, regardless of the analysis method or entrainment mechanism, agrees that mold flux entrainment depends mainly on the physical properties of the materials involved (especially the density, viscosity, and interfacial tension of the steel and slag); the slag layer thickness; and the flow system design and operating conditions (especially nozzle geometry, casting speed, and argon gas flow rate).

Flux entrainment has received much attention over the years and several mechanisms have been proposed, which are summarized in this work. Many studies have used room-temperature physical models, usually with water and a silicon oil. Physical models are unable to match all of the relevant similarity criteria simultaneously, however, so their results are difficult to interpret quantitatively. The ever-advancing computer technology has also allowed numerical investigations of flux entrainment, although challenges related to turbulent and multiphase flow still remain. The computational models referred to in this paper usually treat turbulence with the $k-\varepsilon$ model, though other models find occasional use.

Previous reviews of work on this topic include those of Herbertson *et al.*[1], Suzuki *et al.*[2], and Thomas[3], but a comprehensive picture of the mechanisms of mold flux entrainment remains elusive. Early work focused mainly on fluctuations of the meniscus level, which correlate strongly with defects. The entrainment mechanisms reported in later literature fall into eight more families: meniscus freezing, argon bubble interaction, slag "crawling" down the submerged entry nozzle (SEN), vortexing, meniscus standing wave instability, shear-layer (Kelvin-Helmholtz) instability, narrow face spout impingement upon the meniscus, and meniscus balding. Most mechanisms suggest a critical condition for entrainment, which can be used as a practical evaluation of physical or numerical models of fluid flow in a caster.

Entrainment is not detrimental to product quality unless the inclusions ultimately become caught in the solidifying steel. Particles may or may not become entrapped in an approaching dendritic solidification front depending on the particle diameter, local crossflow velocity, and steel composition[4]. Downward flow velocities may exacerbate entrapment by suspending the rising particles in front of the solidifying interface[5], which may explain why single-roll patterns are found to produce more slag entrapment defects[6]. The capacity of the liquid slag layer to absorb the inclusions that reach it depends greatly on the composition, and associated properties[7]. Dynamic models have been constructed for solid[8] and liquid[9] particles to determine if a particle will be absorbed into the slag layer, which decreases with

decreasing inclusion particle diameter, decreasing wettability between the slag and particles, increasing interfacial tension, and increasing slag viscosity. However, these same properties which discourage inclusion removal often help to prevent entrainment from occurring at all.

This paper presents a critical overview of the nine families of mechanisms that cause entrainment of mold slag during continuous casting. The review adopts the following symbols: V is velocity, g is acceleration due to gravity, μ is molecular viscosity, ρ is density, and Γ_{AB} is interfacial tension between fluids A and B. The subscript u refers to the upper fluid layer (melted mold powder) and the subscript l refers to the lower fluid layer (molten steel). SEN port angles are defined to increase when pointing less steeply downwards.

2 Meniscus level fluctuations

Many early studies on slag entrainment mechanisms focused on transient fluctuations of the meniscus, because they are observable and measurable in the steel plant. However, recent numerical models[10,11] showed how level fluctuations can entrain slag by exposing the dendritic interface of the top of the solidifying steel shell to liquid slag and mold powder during a sudden drop in the level. Fig. 1 shows the sequence of events leading to entrainment by this mechanism. Although oscillation causes slight changes in liquid level during each cycle, transient changes in the flow pattern in the mold are responsible for the large level fluctuations that cause severe slag entrainment defects.

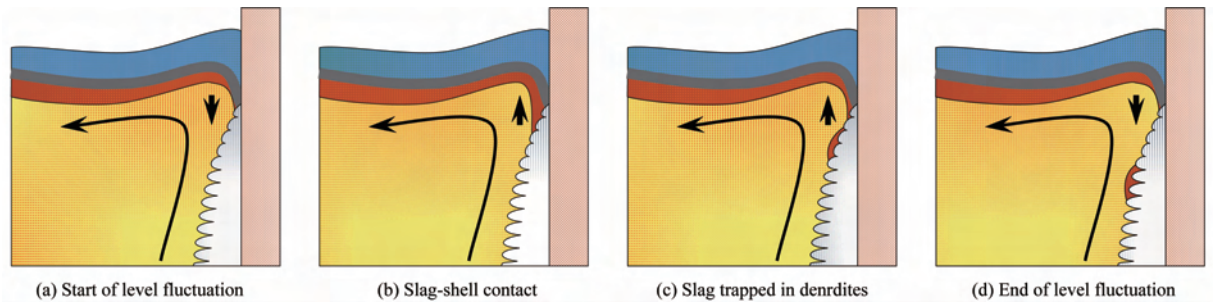

Fig. 1 Entrainment by meniscus level fluctuation

Physical model studies have shown that meniscus fluctuations increase with increasing casting speed[12,13], increasing SEN bore diameter[14], increasing (ie. more upwards) SEN port angles[12,14], decreasing SEN immersion depth[12], decreasing slab width[12], and increasing argon flow rate[12,14,15]. Poor wettability between the argon and SEN refractory increases the effect of argon on fluctuations[15], but increasing the casting speed decreases the effect of argon bubbles[12]. Electromagnetic forces offer another variable to control the flow pattern. Plant experiments using electromagnetic braking have reported decreases in level fluctuations and associated defects (cf. the review in the paper by Cukierski and Thomas[16]).

3 Meniscus freezing and hook formation

Another mechanism for the entrainment of slag and inclusion particles to form surface defects is illustrated in Fig. 2, which shows a slag particle entrapped by a hook. The root cause of hook formation[17,18] is freezing of the meniscus, due to insufficient heat delivered to the meniscus region near the narrow face. The frozen meniscus may extend into the melt and capture rising bubbles or particles. In addition, overflowing of the frozen meniscus can entrap any slag coating its surface. Hooks can be prevented by increasing flow velocity, increasing superheat, or increasing SEN port angles more upwards, all of which increase the heat supply to this region.

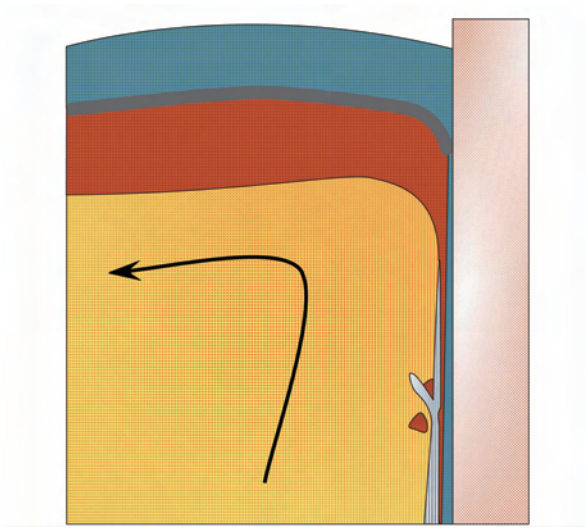

Fig. 2 Hook trapping a particle

Flow conditions such as caused by a shallow SEN may produce excessive meniscus surface velocities which increase surface turbulence, leading to instability, entrapment, and uneven powder distribution, as discussed in the previous section.

However, too deep an SEN can result in meniscus freezing, hook formation, and shell thinning below mold exit[19]. Kubota[13] demonstrated that EMBr may be used to increase flow velocities at lower casting speeds to avoid hook formation, and gave the condition that surface velocities should be kept above a lower limit of 0.15 – 0.25 m/s to minimize surface defects for the mold considered in the study.

4 Argon bubble interactions

Argon gas is usually fed into the SEN to help prevent nozzle clogging, which leads to problems from both nonmetallic inclusions and asymmetric fluid flow. Argon bubbles also add a buoyancy force to the steel flow that changes the flow pattern. Thus, argon injection may lessen some problems, such as hook formation, but is detrimental to other entrapment mechanisms, such as surface level fluctuations.

Emling, *et al.*[20] found product defects caused by argon gas bubbles coated with mold slag. They noted in a water model study that argon bubbles flowing out of the SEN can form a foam with the slag layer, which can adhere to and crawl down the outside of the nozzle and become caught in the nozzle jet, as illustrated in Fig. 3. The occurrence of the foam was found to increase with increasing slab width, increasing argon injection rate, increasing slag viscosity, decreasing slag density, and decreasing interfacial tension between the slag and steel[20]. A critical maximum argon flow rate was observed to reduce defects[20], and was later shown[15] to increase with decreasing casting speed, increasing slag layer viscosity, increasing nozzle port angles, and increasing wettability between the SEN refractory and molten slag.

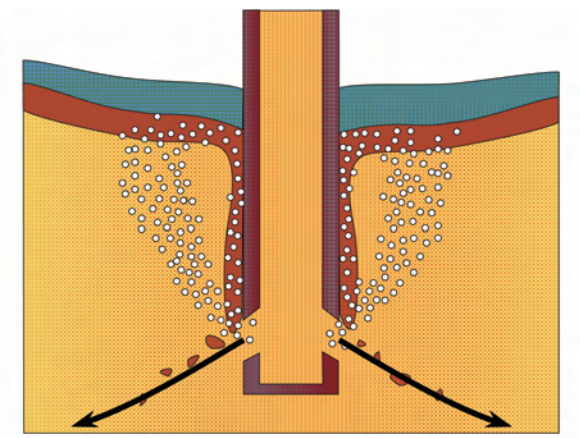

Fig. 3 Slag foaming

5 Slag crawling

A solid object submerged into a flowing liquid will result in a pressure buildup on the windward (right) side and a corresponding pressure drop in the leeward (left) side, as illustrated in Fig. 4(a). When a free surface is present, these pressure changes will cause changes in elevation of the surface. Asymmetric flow in a continuous casting mold can cause this situation to occur. This low-pressure zone might draw some liquid slag down along the outside of the SEN, and if severe enough, the slag might become entrained into the steel jet and be carried away to form defects, as shown in Fig. 4(b).

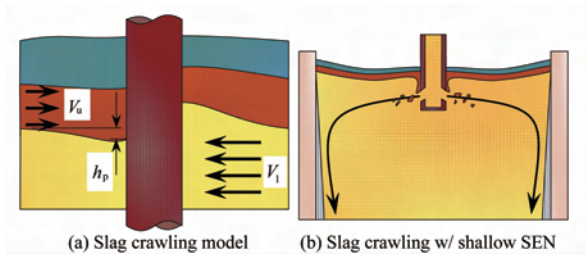

Fig. 4 Slag crawling

Physical model experiments of flow past a circular cylinder[21] were performed to investigate this mechanism. The penetration depth h_p that the upper fluid crawls down the cylinder is:

$$h_p = 1.9[C_{p,max}\rho_u V_u^2 + C_{p,min}\rho_\ell V_\ell^2]/[g(\rho_\ell - \rho_u)] \quad (1)$$

where $C_{p,max} = 1.0$ and $C_{p,min} = 2.5$ are the pressure coefficients for a circular nozzle. For elliptical nozzles, the coefficients to decrease with increasing aspect ratio a according to[22]:

$$C_{p,max} = 1.376 - 0.0652 \cdot a \quad (2)$$

$$C_{p,min} = 1.978 - 1.065 \cdot \ln(a) \quad (3)$$

where the aspect ratio is the ratio of the major diameter (parallel to the flow direction) to the minor diameter, so increasing the SEN aspect ratio lowers the penetration depth. To avoid entrainment by this mechanism, the SEN immersion depth should be greater than the slag penetration depth. Note that slag crawling and the slag foaming mechanism discussed previously can act together to aggravate entrainment[20], but this is not reflected in Eq. (1).

6 Von kármán vortex formation

Flow past bluff bodies can result in the periodic shedding of vortices in the wake of the object. Asymmetric flow between sides of the mold is the source of flow through the narrow gap between the SEN and mold walls that causes vortices that entrain slag, as shown in Fig. 5. The slightest asymmetry can result in the formation of vortices, but this does not guarantee the entrainment of slag.

These vortices can entrain slag that becomes entrapped between the dendrites on the wide face

near the SEN, leading to a sharp increase in the number of sliver defects in the center of the slabs[19]. Alternatively, vortices may pull a funnel of slag deep enough into the mold that the jet coming out of the SEN entrains the tip of the vortex, transporting slag-related inclusions elsewhere in the slab[23－25]. The vortices are always observed to form on the weaker side of the flow, *i. e.* in the wake of the SEN[23－29]. Vortex depth increases with increasing meniscus surface velocity[23,27]. Vortex diameter increases with increasing casting speed[23] and SEN misalignment[23,24]. Vortex formation frequency increases with increasing slab width[19,28], shallower SEN immersion depths[19,25,28], increasing SEN port angle[24,25], increasing casting speed[19,23－25,27], and increasing SEN misalignment[23,24].

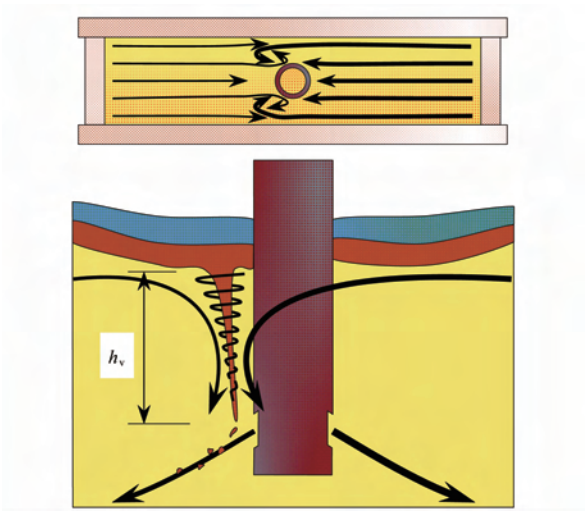

Fig. 5 Vortexing entrainment

Vortex formation needs both rotational flow in the plane of the meniscus, and a downward-pulling sink. The sink momentum is found where the opposing roll flows meet near the center of the mold[26,27]. A maximum velocity for vortex formation was also observed, because excessive velocities cause the meniscus to become too oscillatory and turbulent to allow the formation of vortices[25,27]. Computational models confirm that vortex formation cannot occur with perfectly symmetric geometry and flow conditions[23,30]. Meeting a critical meniscus velocity or flow rate criterion does not guarantee vortex formation[28], and furthermore, the presence of a vortex does not necessarily mean that slag will be entrained into the melt[25].

Increasing argon flow rates to above 10% gas fraction induces buoyancy that can decrease the downward velocity near the SEN and prevent vortex formation, but this reinforces asymmetric flow[23] and can also trigger the argon-related mechanisms discussed above. Vortex formation was shown to be effectively suppressed with sufficiently strong EMBr to control the asymmetry of the flow[23,29]. Recent water modeling[25] has proposed a critical surface velocity for vortex formation of 0.3 m/s, as well as a model to predict the depth of vortices h_v:

$$h_v = [V_{mc}^2/g][\rho_\ell/(\rho_\ell - \rho_u)] + c([\Delta V_s^2/g][\rho_u/(\rho_\ell - \rho_u)])^{0.55} \quad (4)$$

where V_{mc} is the horizontal steel velocity (m/s) in the center of the mold, 10 mm below the water-oil interface and halfway between the SEN and wide face, ΔV_s is the sudden change in vertical velocity, measured 50 mm below the steel-slag interface, 10 mm away from the SEN and halfway between the wide faces, and $C = 0.0562m^{0.45}$ is a constant with all other quantities in m-kg-s units. This model predicts the SEN immersion depth needed to avoid the jets cutting of the tips of the vortices.

7 Meniscus standing wave instability

Flow beneath a free liquid surface will create surface waves which can become unstable and turn over to entrain the interface, if the local slope becomes sufficiently steep (exceeding vertical)[31]. The flow in continuous casting molds leads to a stationary wave in the surface shape, excluding the local level fluctuations discussed previously. A stability criterion was proposed as a height-to-wavelength ratio[31,32]:

$$(h_{wave}/\lambda)_{crit} = 0.21 + 0.14(\rho_u/\rho_\ell)^2 \quad (5)$$

where h_{wave} is the wave height defined as the vertical distance between the lowest point (trough) and highest point (crest) of the surface level and is the wavelength, defined as the distance between the outer SEN wall and the narrow faces[32－34]. Early experiments indicated this model is an overprediction and that a vortex forms at the node at lower height-to-wavelength ratios, indicating that the stability of the wave is governed by shearing at the interface, rather than by the wave turning over[31].

Eq. 6 can be used with any of the models available in the literature[28,32,33,35,36] that predict the wave height to create a criterion for critical SEN port velocity. For example, the wave height h_{wave} may be calculated as[32]:

$$h_{wave} = 0.31(V_{port}^2/g)(D_{port}/L_c) \cdot [(\rho_\ell + \rho_u)/(\rho_\ell - \rho_u)] \quad (6)$$

where D_{port} is the diameter of the SEN ports, V_{port} is the velocity of the molten steel at the SEN ports, and L_c is a characteristic length taken as the height of the upper recirculation zone, calculated as $L_c = h_{SEN} + \frac{1}{2}w_{slab}\tan(\phi_{discharge} - \frac{1}{2}\phi_{jet})$ for immersion

depth h_{SEN}, slab width w_{slab}, jet discharge angle $\phi_{discharge}$, and jet spread angle ϕ_{spread}, as shown in Fig. 6.

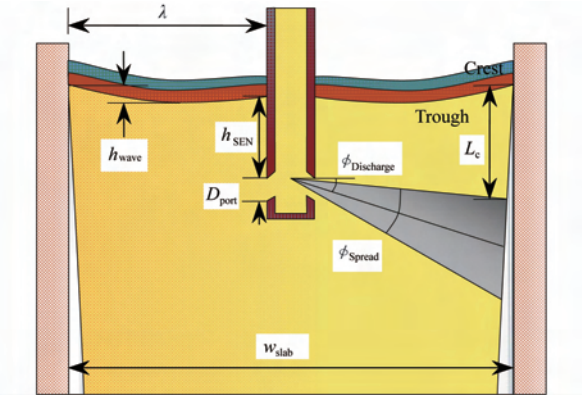

Fig. 6 Standing wave instability

With a proper surface tension model, the wave instability event was successfully simulated numerically[37]. This numerical model showed a recirculating packet of fluid at the trough that disappeared after entrainment. This suggests that shear stresses form a horizontal vortex that causes the instability of the interface, which is a different mechanism, discussed in the next section. The highest surface velocities coincide with the trough of the standing wave[34,37,38], which again indicate that shear instability is the real cause of entrainment. None of the models in the literature investigated a steel-slag system, asymmetry effects, or combined effects of buoyancy, surface tension, and three-dimensional flow features. However, it appears likely that the standing wave height instability (turnover) mechanism is not a problem in practice, because shear instability occurs more easily.

8 Shear layer instability

The interface between two density-stratified fluids with relative motion will become unstable with a large-enough difference in velocity. A theoretical condition for this instability was derived by Helmholtz[39] and Kelvin[40] for two idealized fluids separated by a flat interface. Most researchers have identified shear instability of the interface to be a cause for mold slag entrainment, shown in Fig. 7, though little has been done to explore this mechanism. This fundamental hydrodynamic phenomenon of Kelvin-Helmholtz instability has received considerable treatment over the last 150 years and is found throughout nature, including ocean waves and clouds. The interface between the two fluids becomes unstable when the velocity difference between the two layers is greater than:

$$\Delta V_{crit} = \sqrt[4]{4g(\rho_\ell - \rho_u)\Gamma_{ul}[\rho_u^{-1} + \rho_\ell^{-1}]^2} \quad (7)$$

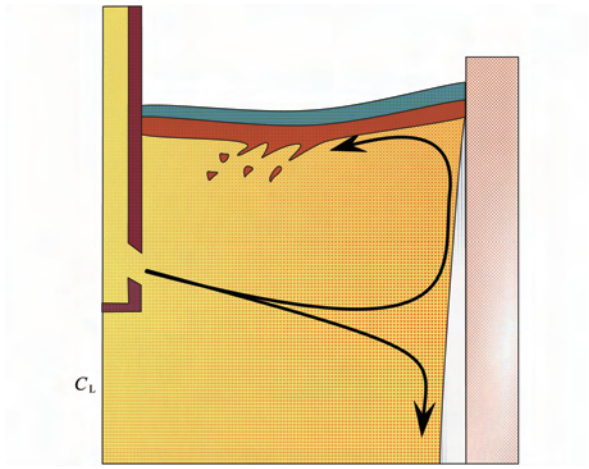

Fig. 7 Shear instability

Magnetic fields applied transverse to the flow direction do not affect the stability of the interface, and fields applied parallel to the flow direction have the same effect as surface tension in stabilizing the interface[41]. The physical model experiments of Iguchi, *et al.*[42] confirmed the Milne-Thomson[43] extension of the Kelvin-Helmholtz theory for finite-depth fluids using low-viscosity oils, where surface tension is not important. This shear instability mechanism is most likely to occur midway between the narrow face and the SEN where the horizontal surface velocity is a maximum.

9 Upward flow impinging on meniscus

The upward spout along the narrow faces resulting from a double-roll flow pattern may cause slag entrainment in both cutting[20] and dragging[44] and modes, illustrated in Figs. 8 and 9. This is an example of shear-layer instability where the geometric aspects of the flow render the Kelvin-Helmholtz theory inapplicable. Harman and Cramb[44] developed the following relation, based on measurements of oil-and-water model experiments:

$$V_{crit} = 3.065(\Gamma_{ul}^{0.292} g^{0.115}/\delta^{0.365}) \cdot ((\rho_\ell - \rho_u)^{0.215}/\rho_u^{0.694})(\mu_u^{0.231}/\mu_\ell^{0.043}) \quad (8)$$

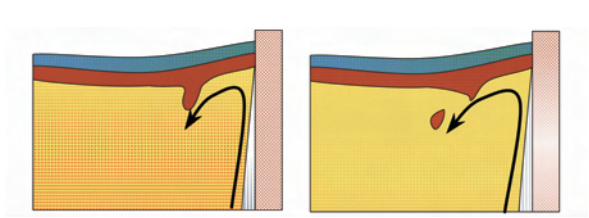

Fig. 8 NF spout, dragging mode

Entrainment occurs more easily with lower water (steel) density, lower interfacial tension, lower oil (slag) viscosity, and increasing slag layer thickness δ. This work was repeated[45] for a wider property

range and more controlled flow patterns and resulted in similar trends, except for the effect of slag layer thickness.

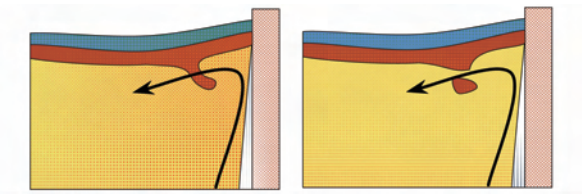

Fig. 9 NF spout, cutting mode

10 Meniscus balding

In a worst-case scenario, some of the above mechanisms for slag entrainment can push the slag layer out of the way, as shown in Figs. 10 and 11. This phenomenon is termed "balding of the meniscus," as it exposes molten steel to the sintered and solid powder layers of the slag layer, if not the atmosphere. This can occur in continuous casting at high nozzle flow rates[38], and the accompanying surface re-oxidation forms inclusions such as alumina. Also, particles of powder can become entrained at the bald meniscus, especially if the bald spot coincides with the trough of the standing wave[38]. Meniscus balding may be prevented by having a slag layer thickness at least the size of the standing wave height[36], such as predicted from Eq. 6. Excessive argon flow rates[46] can also cause balding, as illustrated in Fig. 11.

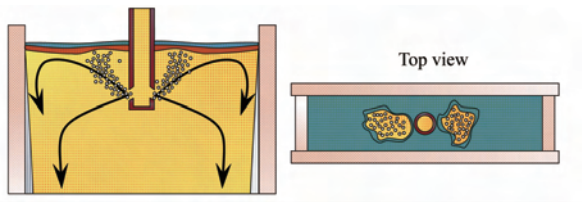

Fig. 10 Balding by excessive NF spout

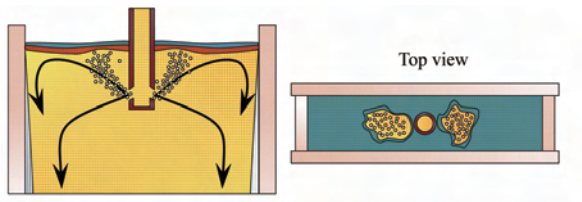

Fig. 11 Balding by excessive argon flow

11 Discussion

Designing and operating a caster to avoid entrainment requires careful selection of many different inter-related parameters, to find a window of stable, entrainment-free operation. Casting conditions must be found to simultaneously avoid each of the above mechanisms. The various equations presented here can be used together as design tools or to help evaluate the results of a numerical or physical model of flow in the caster. In using these equations, it should be noted that critical conditions for a given mechanism are often exceeded due to asymmetric flow conditions, even though symmetric time-averaged flow conditions would have safely avoided entrainment.

There is no single optimum solution. For example, the choice of slag layer properties should balance the conflicting needs to use the slag as an inclusion catcher (requiring lower interfacial tension) with preventing shear instability (requiring high interfacial tension). Further work is needed to include chemical composition and mass transfer effects at the interface[7], which can significantly change the interfacial tensions.

Entrainment by vortex formation combined with related exacerbating mechanisms is likely the most common mechanism of entrainment, owing to the ease at which asymmetric flow can occur. The stability of the standing wave, the impinging narrow face spout, and bone fide Kelvin-Helmholtz instability are all different embodiments of the same mechanism: parallel shear-layer instability. Preventing shear instability requires control of surface velocity. Maintaining a safe surface velocity requires selection of SEN parameters and EMBr settings to avoid excessive meniscus fluctuations and shear instability, while keeping the meniscus temperatures warm enough to prevent hook formation.

12 Conclusion

Many studies have been performed over the years to investigate mold slag entrainment, which is one of the main sources of inclusion defects in continuous casting of steel. This work identifies nine distinct mechanisms responsible for entrainment, especially vortexing due to asymmetric flow, argon bubble interactions with the slag layer, shear-layer instability at the slag-steel interface, and excessive upward flow impingement on the meniscus. Other important mechanisms include meniscus level fluctuations, meniscus freezing and hook formation, and meniscus balding. Standing wave instability appears unlikely as shear-layer instability can occur more easily. The slag layer can also crawl down the SEN, which is important at shallow submergence depths or with slag foaming. The various simple models available to estimate these nine mechanisms are summarized here, and can be used together to evaluate flow patterns in models of the flow field in the molten steel pool. Predictions are further complicated, because the different mechanisms can act together to aggravate entrainment. Much future work is needed to develop

better prediction tools to control this important problem.

Acknowledgements

The authors gratefully acknowledge the financial support of the member companies of the Continuous Casting Consortium at the University of Illinois.

References

[1] Herbertson J, He Q L, Flint P J, *et al*. Modelling of metals delivery to continuous casting moulds[C]// 74th Steelmaking Conf. Proc. ,1991:171-185.

[2] Suzuki M and Nakada M. Perspectives of research on high-speed conventional slab continuous casting of carbon steels[J]. ISIJ Int. ,2001,41(8):670-682.

[3] Thomas B G. Modeling of continuous-casting defects related to mold fluid flow[C]// Proc. 3rd Int. Cong. Sci. Tech. Steelmaking,2005:847-861.

[4] Yuan Q and Thomas B G. Transport and entrapment of particles in continuous casting of steel[C]// Proc. 11th Modeling of Casting, Welding, Advanced Solidification Processes,2006:745-752.

[5] Lee G-G, Shin H-J, Thomas B G, *et al*. Asymmetric multi-phase fluid flow and particle entrapment in a continuous casting mold[C]// Proc. AISTech 2008: 63-73.

[6] Kunstreich S and Dauby P H. Effect of liquid steel flow pattern on slab quality and the need for dynamic electromagnetic control in the mould[J]. Ironmaking Steelmaking,2005,32(1):80-86.

[7] Cramb A W, Chung Y, Harman J, *et al*. The slag/ metal interface and associated phenomena[J]. Iron Steelmaker,1997,24(3):77-83.

[8] Bouris Dand Bergeles G. Investigation of inclusion re-entrainment from the steel-slag interface[J]. Metall. Met. Trans. B,1998,29(3):641-649.

[9] Strandh J, Nakajima K, Eriksson R. *et al*. A mathematical model to study liquid inclusion behavior at the steel-slag interface[J]. ISIJ Int. , 2005,45(12):1838-1847.

[10] Ojeda C, Thomas B G, Barco J, *et al*. Model of thermal-fluid flow in the meniscus region during an oscillation cycle[C]// Proc. AISTech 2007: 269-283.

[11] Sengupta J, Ojeda C and Thomas B G. Thermal-mechanical behaviour during initial solidification in continuous casting:steel grade effects[J]. Int. J. Cast Metals Res. ,2009,22(1-4):8-14.

[12] Teshima T, Osame M, Okimoto K, *et al*. Improvement of surface property of steel at high casting speed[C]// 71st Steelmaking Conf. Proc. , 1988:111-118.

[13] Kubota J, Okimoto K, Shirayama A, *et al*. Meniscus flow control in the mold by travelling magnetic field for high speed slab caster[C]// 74th Steelmaking Conf. Proc. ,1988:233-241.

[14] Nakato H, Saito K, Oguchi Y, *et al*. Surface quality improvement of continuously cast blooms by optimizing solidification in early stage[C]// 70th Steelmaking Conf. Proc. ,1987:427-431.

[15] Wang Z, Mukai K, Ma Z, *et al*. Influence of injected ar gas on the involvement of the mold powder under different wettabilities between porous refractory and molten steel[J]. ISIJ Int. ,1999,39(8):795-803.

[16] Cukierski K and Thomas B G. Flow control with local electromagnetic braking in continuous casting of steel slabs[J]. Metall. Met. Trans. B, 2008, 39 (1):94-107.

[17] Sengupta J, Thomas B G, Shin H-J, *et al*. A new mechanism of hook formation during continuous casting of ultra-low-carbon steel slabs[J]. Metall. Met. Trans. A,2006,37(5):1597-1611.

[18] Lee G-G, Thomas B G, Kim S-H, *et al*. Microstructure near corners of continuous-cast steel slabs showing three-dimensional frozen meniscus at hooks[J]. Acta Mat. ,2007,55(20):6705-6712.

[19] WangY H. A study of the effect of casting conditions on fluid flow in the mold using water modelling[C]// 73rd Steelmaking Conf. Proc. ,1990:473-480.

[20] Emling W H, Waugaman T A, *et al*. Subsurface mold slag entrainment in ultra low carbon steels[C]// 77th Steelmaking Conf. Proc. ,1994:371-379.

[21] Yoshida J, Ohmi T and Iguchi M. Cold model study on the effects of density difference and blockage factor on mold powder entrainment[J]. ISIJ Int. , 2005,45(8):1160-1164.

[22] Ueda Y, Kida T and Iguchi M. Unsteady pressure coefficient around an elliptic immersion nozzle[J]. ISIJ Int. ,2004,44(8):1403-1409.

[23] Li B, Okane T, and Umeda T. Modeling of biased flow phenomena associated with the effects of static magnetic-field application and argon gas injection in slab continuous casting of steel[J]. Metall. Met. Trans. B,2001,32(6):1053-1066.

[24] Li B and Tsukihashi F. Vortexing flow patterns in a water model of slab continuous casting mold[J]. ISIJ Int. ,2005,45(1):30-36.

[25] Kasai N and Iguchi M. Water-model experiment on melting powder trapping by vortex in the continuous casting mold[J]. ISIJ Int. ,2007,47(8):982-987.

[26] He Q. Observations of vortex formation in the mould of a continuous slab caster[J]. ISIJ Int. , 1993, 33 (2):343-345.

[27] Gebhard M, He Q L and Herbertson J. Vortexing phenomena in continuous slab casting moulds[C]// 76th Steelmaking Conf. Proc. ,1993:441-446.

[28] Gupta D and Lahiri A K. Water-modeling study of the surface disturbances in continuous slab caster [J]. Metall. Met. Trans. B,1994,25(2):227-233.

[29] Li B and Tsukihashi F. Effects of electromagnetic brake on vortex flows in this slab continuous casting mold[J]. ISIJ Int. ,2006,46(12):1833-1838.

[30] Kastner G, Brandstätter W, Kaufmann B, *et al*. Numerical study on mould powder entrapment caused by vortexing in a continuous casting process[J]. Steel Res. Int. ,2006,77(6):404-408.

[31] Rottman J W. Steep standing waves at a fluid interface[J]. J. Fluid Mech. ,1982,124:283-306.

[32] Theodorakakos A and Bergeles G. Numerical investigation of the interface in a continuous steel casting mold water model[J]. Metall. Met. Trans. B, 1998,29(6):1321-1327.

[33] Panaras G A, Theodorakakos A and Bergeles G. Numerical investigation of the free surface in a continuous steel casting mold[J]. Metall. Met. Trans. B,1998,29(5):1117-1126.

[34] Anagnostopoulos J and Bergeles G. Three-dimensional modeling of the flow and the interface

surface in a continuous casting mold model [J]. Metall. Met. Trans. B, 1999, 30(6): 1095-1105.
[35] Moghaddam B S, Steinmetz E and Scheller P R. Interaction between the flow condition and the meniscus disturbance in the continuous slab caster [C] // Proc. 3rd Int. Cong. Sci. Tech. Steelmaking, 2005: 911-920.
[36] Gupta D and Lahiri A K. Cold model study of the surface profile in a continuous slab casting mold: effect of second phase [J]. Metall. Met. Trans. B, 1996, 27(4): 695-697.
[37] Dash S K, Mondal S S and Ajmani S K. Mathematical simulation of surface wave created in a mold due to submerged entry nozzle [J]. Int J Num Meth Heat Fluid Flow, 2004, 14(5): 606-632.
[38] Gupta D and Lahiri A K. Cold model study of slag entrainment into liquid steel in continuous slab caster [J]. Ironmaking Steelmaking, 1996, 23(4): 361-363.
[39] von Helmholtz H L F. Über discontinuierliche Flueßigkeits-Bewegungen. Monatsb. K. Preuss. Akad. Wiss. Berlin, 1868, 23: 215-228.
[40] Thomson (Lord Kelvin) W. Hydrokinetic solutions and observations [J]. Phil Mag, 1871, 42(281): 362-377.
[41] Cha P and Yoon J. The effect of a uniform direct current magnetic field on the stability of a stratified liquid flux/molten steel system [J]. Metall Met Trans B, 2000, 31(2): 317-326.
[42] Iguchi M, Yoshida J, Shimizu T, *et al*. Model study on the entrapment of mold powder into molten steel [J]. ISIJ Int, 2000, 40(8): 685-691.
[43] Milne-Thomson L M. Theoretical Hydrodynamics, 5e. Macmillan Press, London, 1968.
[44] Harman J M and Cramb A W. A Study of the Effect of Fluid Physical Properties upon Droplet Emulsification [C] // Proc. 79th Steelmaking Conf., 1996: 773-784.
[45] Savolainen J, Fabritius T and Mattila O. Effect of fluid physical properties on the emulsification [J]. ISIJ Int, 2009, 48(1): 29-36.
[46] Harris D J and Young J D. Water Modeling-A Viable Production Tool [C] // Proc. 65th Steelmaking Conf, 1982: 3-16.